

Article

Not peer-reviewed version

Effect of Experimental Parameters on Cavitation Dose in Ultrasonic Baths via Modified Aluminum Foil Test

[Svetlana Saikova](#)*, Diana Nemkova, [Anton Krolikov](#)

Posted Date: 25 February 2026

doi: 10.20944/preprints202602.1405.v1

Keywords: sonication; dispersion; aluminum foil; cavitation erosion; solvent properties



Preprints.org is a free multidisciplinary platform providing preprint service that is dedicated to making early versions of research outputs permanently available and citable. Preprints posted at Preprints.org appear in Web of Science, Crossref, Google Scholar, Scilit, Europe PMC.

Copyright: This open access article is published under a [Creative Commons CC BY 4.0 license](#), which permit the free download, distribution, and reuse, provided that the author and preprint are cited in any reuse.

Disclaimer/Publisher's Note: The statements, opinions, and data contained in all publications are solely those of the individual author(s) and contributor(s) and not of MDPI and/or the editor(s). MDPI and/or the editor(s) disclaim responsibility for any injury to people or property resulting from any ideas, methods, instructions, or products referred to in the content.

Article

Effect of Experimental Parameters on Cavitation Dose in Ultrasonic Baths via Modified Aluminum Foil Test

Svetlana Saikova ^{1,2,*}, Diana Nemkova ^{1,2} and Anton Krolikov ²

¹ School of Non-Ferrous Metals, Siberian Federal University, Svobodny, 79, 660041 Krasnoyarsk, Russia

² Institute of Chemistry and Chemical Technology, Federal Research Center "Krasnoyarsk Science Center of the Siberian Branch of the Russian Academy of Sciences", Akademgorodok, 50/24, 660036 Krasnoyarsk, Russia

* Correspondence: ssaikova@sfu-kras.ru

Abstract

Ultrasonic cavitation is a key mechanism in the dispersion and erosion of solid materials in liquids; however, the influence of processing conditions and medium properties on its efficiency in ultrasonic baths remains poorly systematized. Despite the widespread use of ultrasonic baths in materials processing, general optimization principles are lacking, and operating parameters are typically determined empirically for each system. In this work, cavitation activity was quantitatively assessed using an aluminum foil erosion test, with the foil clamped in a plastic frame to evaluate the mechanical effects of cavitation. The effects of ultrasonic power, frequency, treatment time, temperature, solvent nature, and vessel material on the foil mass loss were systematically investigated. The results demonstrate that both the instrumental parameters and physicochemical properties of the dispersion medium, including viscosity and surface tension, significantly affect the cavitation activity. Solvents with lower cavitation thresholds and favorable acoustic properties promote more intense erosion, while the vessel material and geometry also influence energy transmission to the liquid. This study provides a systematic framework for assessing the cavitation dose in ultrasonic baths and offers practical guidelines for optimizing ultrasonic dispersion processes and improving their reproducibility.

Keywords: sonication; dispersion; aluminum foil; cavitation erosion; solvent properties

1. Introduction

Ultrasonic irradiation of liquids generates a variety of physical and chemical effects, including heating, mixing and the formation of transient microscopic hotspots that can drive high-energy reactions [1–3]. Two principal modes of ultrasound delivery are commonly employed: direct (via a sonotrode or ultrasonic probe) [4–12] and indirect (via an ultrasonic bath) [13–17].

Direct sonication typically relies on a Langevin transducer immersed in the liquid [12]. Acoustic energy is concentrated in the immediate vicinity of the sonotrode tip, enabling efficient dispersion of bulk materials. Several comparative studies have demonstrated the superiority of the probe over the bath for applications such as Cu powder dispersion [16] and biofilm removal [17]. However, prolonged or high-power operation of immersion probes causes significant heating of the medium and erosion of the titanium or aluminum tip, leading to contamination of the product with metallic debris [18].

Indirect sonication, using ultrasonic baths, generates a diffuse, relatively low-intensity cavitation field that is distributed throughout the liquid volume. Although the attainable pressure amplitudes are lower than those achieved near a probe horn, the absence of direct contact between the transducer and the processed medium eliminates both excessive local heating and erosion-related contamination. As a result, ultrasonic baths are particularly attractive for the preparation of high-purity nanomaterials and for applications requiring reproducible treatment of multiple samples.

Ultrasound can promote the formation of nanostructures through two distinct mechanisms: chemical (sonochemical) and physical (mechanical). Sonochemical effects arise from the extreme conditions generated inside collapsing cavitation bubbles, where temperatures of several thousand Kelvin and pressures of hundreds of bar are reached [19]. These conditions induce bond cleavage and enable the synthesis of a wide range of nanostructured materials, including metal oxides such as TiO_2 , ZnO and Fe_3O_4 [6–8,13].

In contrast, physical effects originate from shock waves and high-velocity microjets produced during asymmetric bubble collapse. These mechanical impacts can fragment brittle solids into smaller particles and are widely exploited for the exfoliation and dispersion of layered materials, metals and ceramics [4,5,9,10,14]. For example, probe sonication at 24 kHz has been used to disintegrate Al_3Ti , Al_3V , Si and Al_3Zr crystals [4,5]; gold foil and powder were converted into spherical nanoparticles with sizes of approximately 12–14 nm after prolonged probe sonication [9]; and nanosheets of NiMnO_3 , MoS_2 and Cr_2S_3 were obtained from bulk powders using either ultrasonic probes [10,19,20] or ultrasonic baths [14].

The efficiency of ultrasonic dispersion is governed by the intensity of the shock waves emitted during bubble collapse, which depends on the bubble radius at the moment of implosion [21]. Bubble dynamics are controlled by both the operating parameters of the ultrasonic device, such as frequency and acoustic power [22,23], and the physicochemical properties of the liquid medium, including viscosity, surface tension, vapour pressure and gas solubility [24–27]. Liquids with low viscosity and low surface tension facilitate cavitation at lower energy thresholds; consequently, solvent choice represents a critical, yet often under-reported, experimental variable.

Numerous experimental approaches have been developed to characterize cavitation activity. These include measurements of primary effects, such as pressure and temperature during bubble collapse [4,28,29], as well as secondary effects, including chemical dosimetry based on KI oxidation [25,30–32], sonoluminescence [33–38] and cavitation-assisted dispersion of solid materials [39–44]. KI dosimetry is widely employed owing to its simplicity and good reproducibility; however, it primarily reflects the chemical action of cavitation rather than its mechanical impact. In contrast, the aluminum foil erosion test can provide a direct and quantitative measure of the mechanical action of cavitation, which is the key mechanism responsible for the fragmentation and dispersion of solid particles. This method is simple, inexpensive and enables straightforward visualization of the spatial distribution of cavitation intensity. Under cavitation conditions, thin aluminum foil is perforated within minutes, and the resulting erosion patterns directly map the locations of cavitation foci [44]. Several studies have employed aluminum foil in ultrasonic baths to qualitatively characterize cavitation activity through erosion pattern analysis [40,44–47]. In the present work, we extend this approach by introducing foil mass loss as a quantitative measure of the cavitation dose.

Despite the widespread use of ultrasonic baths in materials processing, systematic investigations into how combined experimental parameters—such as ultrasonic frequency, electrical power, solvent properties, vessel material and temperature—govern the cavitation dose delivered to a sample are still lacking. Moreover, studies on solvent-assisted dispersion typically rely on arbitrary experimental conditions, and systematic comparisons of solvents under identical acoustic and geometrical parameters are rarely performed. This lack of standardization contributes to the well-recognized reproducibility challenges in sonochemistry [39]. To the best of our knowledge, few studies have systematically examined quantitative correlations between cavitation dose in ultrasonic baths and solvent properties under identical acoustic and geometrical conditions.

Here, we address this gap by employing a modified aluminum foil erosion test to quantitatively assess cavitation activity under controlled variation of key experimental parameters. A custom-designed foil holder was developed to position aluminum foil samples perpendicular to the transducer surface, enabling consistent exposure across pressure nodes and antinodes. Foil mass loss was adopted as a robust quantitative metric of cavitation dose. Using two commercial ultrasonic baths operating at 35 and 68 kHz (nominal power density 60 W L^{-1}), we systematically mapped the cavitation field and investigated the influence of ultrasonic frequency, electrical power, exposure

time, liquid temperature, solvent type (water, methanol, ethanol, isopropanol and dimethyl sulfoxide (DMSO)) and vessel material. The resulting dataset establishes clear relationships between solvent properties—vapour pressure, surface tension, viscosity and gas solubility—and the measured cavitation dose, and provides practical guidelines for the rational selection of operating conditions in ultrasonic bath-assisted dispersion processes.

2. Results and Discussion

2.1. Mapping of Cavitation Activity in Ultrasonic Baths

The spatial inhomogeneity of the ultrasonic field in cleaning baths arises from interference between waves reflected from the tank walls and the liquid surface, combined with flexural vibration modes of the tank. These phenomena create a standing wave pattern with distinct regions of high and low acoustic pressure, corresponding to zones of strong and weak cavitation activity [15,37].

To visualize this distribution and identify the optimal sample position for subsequent experiments, cavitation mapping was performed using the aluminum foil erosion test. Pre-weighed foil sheets (12×2.5 cm, thickness $10 \mu\text{m}$) were clamped in a wooden frame and positioned vertically at different locations within each bath. After 5 min of sonication at 25°C and a nominal power density of $60 \text{ W}\cdot\text{L}^{-1}$, the foils were removed, rinsed, dried, and weighed. The mass loss at each position was used as a quantitative measure of local cavitation activity, and the obtained values were interpolated to construct two-dimensional cavitation maps (Figure 1), identifying “hot spots” of strong cavitation and regions of weak or absent activity. Such mapping is essential for optimizing experimental conditions, ensuring reproducibility, and avoiding localized overheating or underexposure.

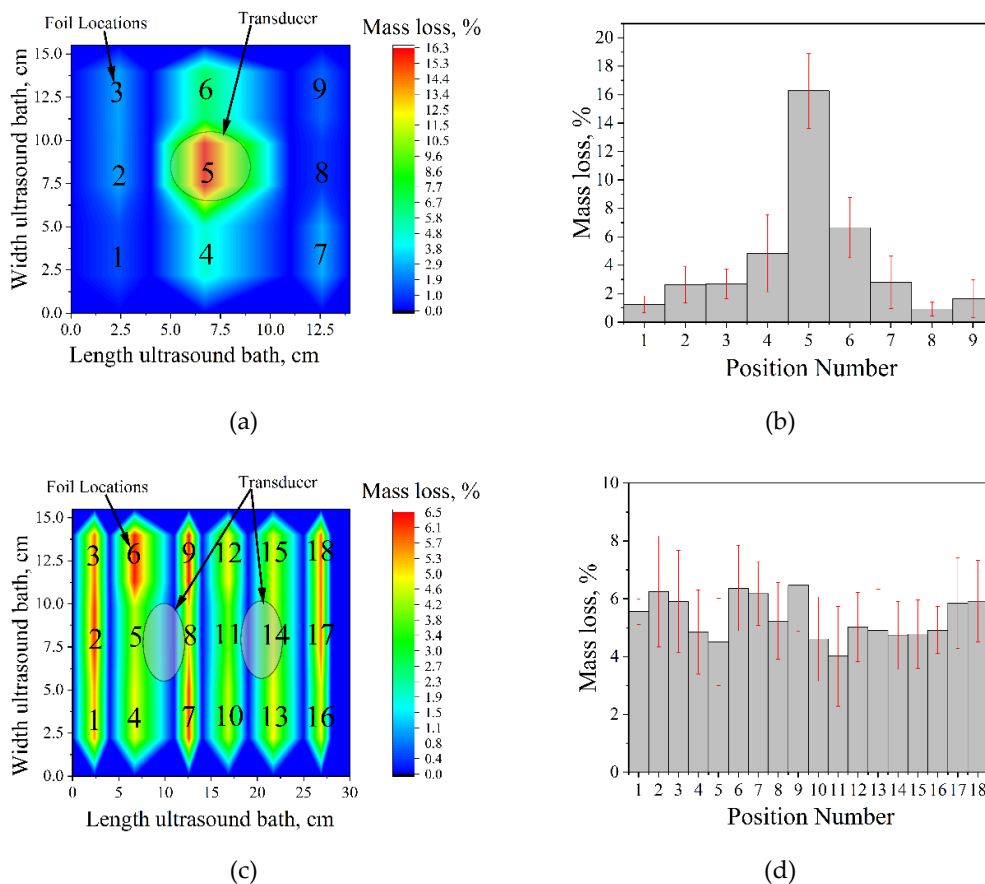


Figure 1. Cavitation maps of ultrasonic baths obtained by aluminum foil erosion after 5 min at 25°C and $60 \text{ W}\cdot\text{L}^{-1}$: (a) spatial distribution of mass loss in the Ultrasonic cleaner (35 kHz); (b) corresponding mass loss profile

as a function of position; (c) spatial distribution in the Vilitex VBS-13DS bath (68 kHz); (d) corresponding mass loss profile.

For the Ultrasonic cleaner (35 kHz; single 45 mm transducer), cavitation activity is strongly concentrated directly above the transducer, with mass loss decreasing sharply with horizontal distance from this hot spot (Figure 1a,b). Accordingly, in all subsequent experiments with this bath, the sample vessel was placed centrally over the transducer.

The Vilitex VBS-13DS bath (68 kHz; two 45 mm transducers) exhibits a considerably more uniform cavitation field, with no pronounced peaks or deep minima across the tested positions (Figure 1c,d). Based on this mapping, the sample was positioned in the geometric center of the bath, equidistant from both transducers. This fixed location, corresponding to the region of highest mechanical cavitation impact, was used throughout all further experiments to ensure reproducible exposure conditions and minimize position-induced variability.

2.2. Effect of the Vessel Material on the Cavitation Dose

The influence of the vessel material on the cavitation dose was investigated using the Ultrasonic cleaner bath (35 kHz; 60 W·L⁻¹) at 25 °C for 5 min. Three cylindrical vessels (150 mL) were tested: two glass vessels (1,2) of different glass types and wall thickness and one polypropylene vessel (3), all filled with 100 mL of distilled water. Their relevant physical properties are summarized in Table 1.

Table 1. Characteristics of vessels* [48,49].

Vessel	Material composition, %	d, mm	E, GPa	β , dB/cm	v, m/s
1	72 SiO ₂ ; 5 Al ₂ O ₃ ; 11 Na ₂ O; 12 B ₂ O ₃	1	48-83	0.01-0.1	5000
2	73 SiO ₂ ; 2 Al ₂ O ₃ ; 15 Na ₂ O; 10 CaO;	3			
3	(C ₃ H ₆) _n	1	1.2-1.6	0.5-3.0	1400-1600

* d - wall thickness; E - Young's modulus; β - attenuation coefficient; v - speed of sound.

The mass loss of aluminum foil was greater in glass vessels than in the polypropylene vessel (Figure 2). Glass, which has a lower attenuation coefficient (typically 0.01-0.1 dB/cm, depending on ultrasound frequency and glass composition) and higher stiffness (elastic modulus 48-83 GPa), transmits ultrasonic energy through the vessel walls more efficiently than polypropylene. The higher stiffness minimizes energy dissipation through wall deformation, while the lower attenuation reduces absorption of acoustic waves within the material, resulting in more effective delivery of cavitation energy to the liquid inside.

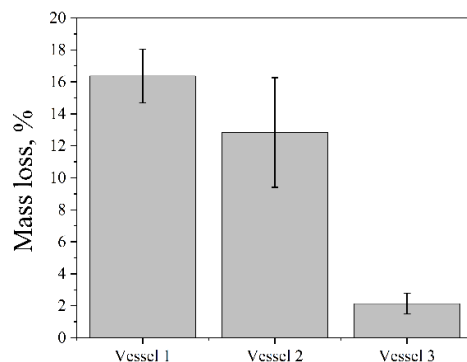


Figure 2. Mass loss of aluminum foil after ultrasonic treatment in vessels of different materials (35 kHz, 60 W·L⁻¹, 25 °C, 5 min).

Thicker walls (vessel 2) increase the acoustic path length, leading to greater energy loss through scattering and absorption within the wall material and consequently reducing sound intensity. It results in lower aluminum foil erosion in vessel 2 compared to vessel 1. Therefore, all subsequent experiments were performed using vessel 1.

2.3. Effect of Ultrasound Frequency and Power on the Cavitation Dose

Table 2 presents the effect of ultrasound frequency on aluminum foil mass loss. The experiments were carried out at 25 °C with a nominal power density of 60 W·L⁻¹ for 5 min. Although different commercial ultrasonic baths were used for these experiments, both systems operated at comparable nominal power densities and under identical experimental conditions, which allows a qualitative comparison of the influence of frequency on the cavitation dose. Increasing the ultrasound frequency from 35 to 68 kHz resulted in an approximately 60% decrease in dispersion efficiency. The observed decrease in mass loss at higher frequency is consistent with the general tendency reported in the literature and is commonly attributed to a substantial reduction in the average cavitation bubble radius with increasing ultrasound frequency [23,36,50]. A smaller maximum bubble radius results in a lower amount of energy accumulated during the expansion stage and, consequently, in a reduced intensity of shock waves generated upon bubble collapse [21].

Table 2. Dependence of aluminum foil mass loss on ultrasonic frequency.

Ultrasonic bath	Frequency, kHz	Mass loss, %
Vilitek VBS-13DS	68	6.4±4.6
Ultrasonic cleaner	35	16.4±1.7

The dependence of aluminum foil mass loss on ultrasonic power was investigated using a Vilitek VBS-4DP ultrasonic bath (68 kHz) at 25 °C for an exposure time of 15 min. With increasing ultrasonic power, the dispersion efficiency increased. A longer sonication time was chosen in this case to ensure measurable foil mass loss over the entire range of applied power densities. The cavitation dose, expressed as foil mass loss, increased from 2.9 ± 0.7% at 20 W·L⁻¹ to 20.9 ± 2.5% at 35 W·L⁻¹ (Figure 3). At power densities above 35 W·L⁻¹, the mass loss reached a plateau, while the standard deviation increased, indicating enhanced temporal and spatial variability of cavitation activity under these conditions. This behavior can be rationalized in terms of changes in bubble population and size with increasing acoustic power. For instance, at 200 kHz, an increase in power from 63.45 to 115.8 W·L⁻¹ was reported to raise the bubble number density from 3.8 × 10¹¹ to 4.92 × 10¹¹ m⁻³ [23]. Similarly, at 1056 kHz, increasing the power from 2 to 10 W resulted in an increase in the average bubble radius from 1.8 to 4.5 μm [36]. Although these studies were conducted at higher frequencies, they illustrate general trends in the evolution of bubble population and size with increasing acoustic intensity. Further increases in power density did not lead to a significant additional increase in foil mass loss. At high acoustic intensities, the formation of dense cavitation clouds and bubble coalescence can occur, leading to acoustic shielding of the bulk liquid and limiting the effective transmission of ultrasound throughout the volume, thereby hindering further development of cavitation [31,51].

2.4. Effect of Dissolved Gas Concentration on the Cavitation Dose

To investigate the influence of dissolved gas concentration on cavitation activity, three liquid media were prepared: distilled water (control), degassed distilled water, and CO₂-saturated water. Degassed water was obtained by boiling distilled water for 30 min, followed by cooling to room temperature under ambient conditions. CO₂-saturated water was prepared by bubbling carbon dioxide through distilled water at a pressure of 8 atm and a temperature of 15 °C. All experiments were carried out in an Ultrasonic cleaner bath operating at 35 kHz with a nominal power density of 60 W·L⁻¹ at 25 °C for 5 min.

The results are summarized in Table 3. Degassing of the liquid led to a noticeable decrease in the dispersion efficiency, as reflected by the reduced aluminum foil mass loss. This effect is attributed

to the depletion of pre-existing gas nuclei in the liquid, which serve as cavitation nucleation sites. Their absence suppresses bubble formation, resulting in lower cavitation activity and diminished mechanical erosion of the foil [52,53].

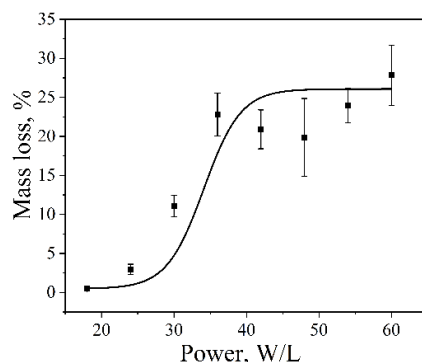


Figure 3. Aluminum foil mass loss as a function of ultrasonic power density in a Vilitek VBS-4DP ultrasonic bath (68 kHz, 25 °C, 15 min).

Table 3. Dependence of aluminum foil mass loss on dissolved gas concentration.

N_0	C_{gases}^* , mmol/L	Mass loss, %
1	<0.01	12.9±3.2
2	0.7	16.4±3.2
3	50	4.1±1.3

* C_{gases} - total concentration of dissolved gases (CO_2 ; O_2 ; N_2).

In contrast, a high concentration of dissolved gas also caused a pronounced decrease in foil mass loss. Under these conditions, the cavitation field is characterized by the formation of a large number of bubbles with a high overall void fraction. Such bubble populations efficiently scatter and absorb the incident ultrasonic waves, leading to acoustic shielding of the bulk liquid and a reduction in the effective cavitation intensity available for erosion [54]. As a result, the dependence of aluminum foil mass loss on dissolved gas concentration exhibits a non-monotonic character, with a maximum at moderate gas concentrations.

2.5. Effect of Ultrasonic Treatment Time on the Cavitation Dose

The influence of ultrasonic treatment time on the cavitation dose was investigated using an Ultrasonic cleaner bath operating at 35 kHz with a nominal power density of $60 \text{ W} \cdot \text{L}^{-1}$ at 25 °C. With increasing sonication duration, the dispersion efficiency increased progressively. The dependence of aluminum foil mass loss on treatment time exhibited a complex, two-stage character (Figure 4).

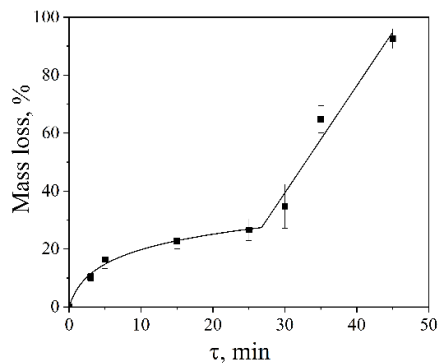


Figure 4. Aluminum foil mass loss as a function of ultrasonic treatment time (Ultrasonic cleaner, 35 kHz, 60 W·L⁻¹, 25 °C). Two distinct regimes are observed: logarithmic growth (3–30 min) and linear behavior (>30 min).

In the initial stage (3–30 min), the foil mass loss increased in a logarithmic manner, from 10 ± 1% to 34 ± 7%. In this regime, the dominant mechanism of material degradation is associated with fatigue-related processes resulting from repeated mechanical loading of the solid surface by shock waves and microjets generated during cavitation bubble collapse [4,5]. Such cyclic stresses promote the gradual growth of pre-existing cracks and structural defects until a critical size is reached, ultimately leading to brittle fracture of the foil.

After approximately 30 min of ultrasonic treatment, the erosion behavior transitioned to a linear regime. At this stage, progressive disintegration at the foil edges caused the sample to detach from the holder and disperse into the bulk liquid as freely suspended fragments (Figure 5). This change in the physical state of the sample—from a fixed foil to mobile fragments—modifies the erosion mechanism and accounts for the observed linear dependence of mass loss on treatment time.

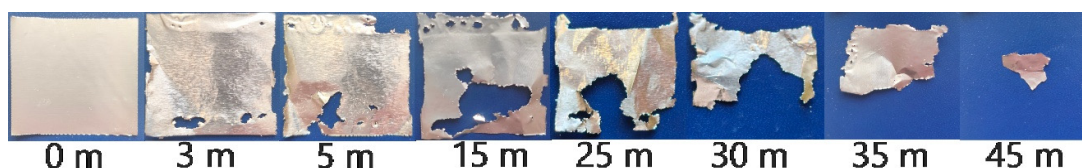


Figure 5. Photographs of aluminum foil samples after ultrasonic treatment for 3 to 45 min, illustrating progressive erosion and eventual disintegration of the foil.

It should also be noted that prolonged sonication at extended treatment times (typically beyond 15–20 min) led to increased variability in the experimental results. This behavior is attributed to partial overheating of the liquid and fluctuations in transducer performance, which can destabilize the cavitation field and affect the reproducibility of cavitation-induced erosion during long-term operation of ultrasonic baths.

2.6. Effect of Solvent Temperature on the Cavitation Dose

The influence of solvent (water) temperature, while keeping all ultrasonic operating parameters constant, on the efficiency of ultrasonic dispersion of aluminum foil was investigated using an Ultrasonic cleaner operating at 35 kHz with a nominal power density of 60 W·L⁻¹ for 5 min. The results revealed a non-monotonic dependence of foil mass loss on temperature, with pronounced maxima at 15 °C and 65 °C and a minimum in the intermediate range of 35–55 °C (Figure 6). Such behavior arises from the simultaneous variation of several physicochemical properties of the liquid that govern cavitation processes (Table 4).

At lower temperatures (e.g., 15 °C), increased surface tension and viscosity of water are accompanied by higher concentrations of dissolved gases and lower saturated vapor pressure. These conditions favor the formation of cavitation bubbles capable of growing to larger radii in the acoustic field. For such bubbles, the mechanical energy released upon collapse is maximized, provided that supersaturation with the vapor phase remains limited, resulting in a more pronounced mechanical impact on the solid surface [51].

Table 4. Physical properties* of water at various temperatures.

T, °C	ρ , kg/m ³	P, kPa	σ , mN/m	η , mPa·s
15	999.1	1.7	73.5	1.140
25	997.1	3.2	72.0	0.894
35	994.1	5.6	70.4	0.723
45	990.3	9.6	68.7	0.600

55	985.7	15.8	67.1	0.506
65	981.3	25.0	65.4	0.435
75	975.2	38.9	63.6	0.379

*T – temperature; p – density; P - vapor pressure; σ – surface tension; η – dynamic viscosity.

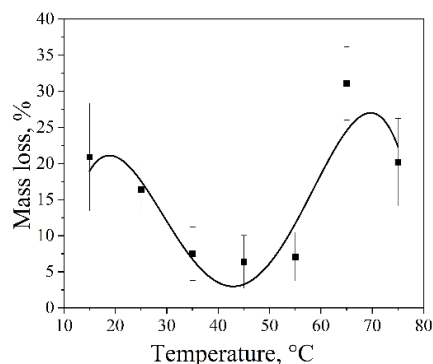


Figure 6. Aluminum foil mass loss as a function of water temperature (Ultrasonic cleaner, 35 kHz, 60 W·L⁻¹, 5 min).

At elevated temperatures (e.g., 65 °C), decreased surface tension and viscosity, together with increased saturated vapor pressure, reduce the cavitation onset threshold and increase the number of cavitation events, which enhances dispersion efficiency. However, at higher temperatures, a rapid increase in vapor pressure leads to a higher vapor content within cavitation bubbles, causing a transition from gaseous to vapor cavitation. This transition damps bubble collapse and reduces its mechanical intensity, thereby decreasing erosion efficiency.

It should be noted that, despite strict control of experimental conditions, the obtained results exhibit pronounced stochasticity, particularly at elevated temperatures. This is reflected in increased data scatter and is associated with the inherently statistical nature of cavitation processes. A similarly complex temperature dependence of aluminum cavitation erosion, along with its stochastic behavior, has been reported previously [55,56].

2.7. Effect of Surface Tension on the Cavitation Dose

To investigate the effect of surface tension on cavitation-induced dispersion, experiments were carried out using aqueous solutions of sodium dodecyl sulfate (SDS) at various concentrations in an Ultrasonic cleaner operating at 35 kHz with a nominal power density of 60 W·L⁻¹ at 25 °C for 5 min (Table 5). As the surface tension of the liquid decreased, the aluminum foil mass loss decreased systematically from 16.4 ± 3.2% to 6.1 ± 2.5%.

Table 5. Effect of sodium dodecyl sulfate solution properties* on aluminum foil mass loss.

C, mol/L	σ , mN/m	η , mPa·s	Mass loss %
1·10 ⁻²	27	0.894	6.1±2.5
1·10 ⁻³	37	0.894	10.7±2.6
1·10 ⁻⁴	49	0.894	14.2±3.5
0	74	0.894	16.4±3.2

*C – concentration SDS; σ – surface tension; η - dynamic viscosity.

Although surfactants are often introduced to facilitate cavitation inception by lowering surface tension, the present results demonstrate that a reduction in surface tension can adversely affect cavitation-induced dispersion efficiency. This behavior can be rationalized in terms of bubble

dynamics. Lower surface tension alters the balance between inertial and surface forces acting on oscillating bubbles, which can promote shape instabilities and bubble fragmentation during the expansion stage. As a result, bubbles may split into smaller daughter bubbles before reaching the critical radius required for inertial collapse [24]. Such premature fragmentation limits the energy accumulated during bubble growth and leads to weaker collapse events, thereby reducing the intensity of shock waves and microjets generated upon collapse [21], which ultimately decreases erosion efficiency.

2.8. Effect of Solvent Properties on the Cavitation Dose

The influence of solvent properties on aluminum foil dispersion was investigated using an Ultrasonic cleaner operating at 35 kHz with a nominal power density of 60 W·L⁻¹ at 25 °C for 5 min. The cavitation dose, expressed as aluminum foil mass loss, increased in the following order: methanol < water < ethanol < DMSO < isopropanol (Figure 7). This non-trivial trend reflects the combined influence of several key physicochemical properties of the solvent, including saturated vapor pressure, surface tension, viscosity, gas solubility, and density (Table 6).

Table 6. Physical properties of solvents* (20 °C) [57–59].

Properties of solvents	Methanol	H ₂ O	Ethanol	DMSO	Isopropanol
T _{b.p.} °C	65	100	78	189	82
C _p , J/(g·K)	2.47	4.18	2.43	1.86	2.59
η, mPa·s	0.8	1.0	1.2	2.5	2.4
σ, mN/m	22.5	72.8	22.4	43.0	21.7
M, g/mol	32	18	46	78	60
ρ, g/cm ³	0.79	0.10	0.79	1.10	0.78
C _{gas} , mM: O ₂ / N ₂	11.1/6.1	1.2/0.7	10.9/6.7	2.5/1.2	10.3/5.9
P, kPa	16.90	3.17	7.87	0.06	6.02

*T_{b.p.} - boiling point solvent; C_p – heat capacity; η - dynamic viscosity; σ - surface tension; M -molar mass; ρ - density solvent; C_{gas} - concentration of dissolved gas; P - vapor pressure.

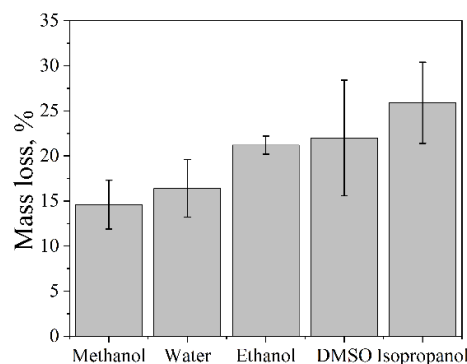


Figure 7. Mass loss of aluminum foil during sonication in various solvents (Ultrasonic cleaner bath, 35 kHz, 60 W·L⁻¹, 25 °C, 5 min).

Methanol exhibited the lowest dispersion efficiency among the solvents studied. This behavior can be primarily attributed to its relatively high saturated vapor pressure, which favors vapor cavitation. In vapor-filled bubbles, a significant fraction of the collapse energy is dissipated through vapor compression, resulting in a pronounced cushioning effect and reduced mechanical impact on the solid surface [51]. Consequently, the erosion of aluminum foil in methanol is limited.

Water displayed an intermediate cavitation dose. Despite its low vapor pressure, which is favorable for energetic bubble collapse, water possesses the highest surface tension and the lowest gas solubility among the investigated solvents. These properties increase the cavitation onset threshold and limit the number of active cavitation nuclei, leading to a lower density of cavitation events and moderate erosion efficiency.

Ethanol demonstrated a higher mass loss compared to both methanol and water. Its lower saturated vapor pressure relative to methanol suppresses vapor cavitation, while its significantly higher gas solubility facilitates the formation of gaseous cavitation bubbles. These conditions promote more intense inertial collapse and enhanced mechanical erosion of the foil.

DMSO showed a further increase in dispersion efficiency. Its surface tension is approximately half that of water, which reduces the cavitation onset threshold and has been correlated with enhanced sonochemical activity [19]. At the same time, the relatively high viscosity of DMSO slows the motion of the bubble wall during oscillation, extending bubble lifetime and potentially increasing the mechanical impulse delivered upon collapse [26]. The combined effect of reduced cavitation threshold and prolonged bubble dynamics results in a higher cavitation dose compared to water and ethanol.

Isopropanol exhibited the highest aluminum foil mass loss among all tested solvents. Its viscosity is comparable to that of DMSO, while its gas solubility is approximately four times higher. The elevated concentration of dissolved gases provides abundant cavitation nuclei during the rarefaction phase of the acoustic cycle, substantially lowering the cavitation onset threshold. In combination with a moderate vapor pressure that limits vapor cushioning, these factors lead to the most intense mechanical cavitation and maximum erosion efficiency.

Additional insight into the cavitation mechanism is provided by the spatial distribution of foil damage within the acoustic field (Figure 8). In several experiments, particularly for ethanol and isopropanol, erosion was strongly localized in regions corresponding to pressure antinodes of the standing ultrasonic wave [15,40]. Such localization is characteristic of mechanically driven cavitation erosion and confirms that shock waves and microjets generated during inertial bubble collapse dominate the dispersion process in these solvents.

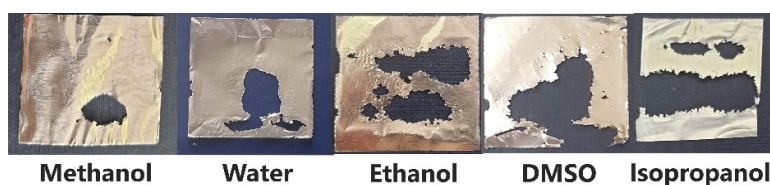


Figure 8. Spatial distribution of aluminum foil erosion patterns after sonication in different solvents, showing localized damage at pressure antinodes.

Based on both cavitation efficiency and practical considerations, isopropanol emerges as the most suitable solvent among those investigated for cavitation-assisted dispersion of aluminum foil.

3. Materials and Methods

3.1. Chemicals

Aluminum foil (thickness 10 μm , GOST 745-2014, RUSAL-Sayanal, Russia), sodium dodecyl sulfate ($\text{CH}_3(\text{CH}_2)_{11}\text{OSO}_3\text{Na}$, $\geq 96\%$, JSC Lenreactiv, Russia), dimethyl sulfoxide ($(\text{CH}_3)_2\text{SO}$, $\geq 99.7\%$, Acros Organics, USA), methanol (CH_3OH , $\geq 99.8\%$, KhimMedService, Russia), ethanol ($\text{C}_2\text{H}_5\text{OH}$, 95%, Konstanta-farm M, Russia), isopropanol ($(\text{CH}_3)_2\text{CHOH}$, $\geq 99.7\%$, Promkhim, Russia). All chemicals were used as received without further purification.

3.2. Cavitation Mapping of Ultrasonic Baths

Pre-weighed aluminum foil sheets (12×2.5 cm) were clamped at the top edge to a wooden frame and positioned vertically in the bath, with the lower edge 10 mm above the bottom and the upper edge at the liquid surface (Figure 9). Ultrasonic treatment was performed for 5 min at a power density of $60 \text{ W}\cdot\text{L}^{-1}$ in the ultrasonic bath (Ultrasonic cleaner (35 kHz; single 45 mm transducer) or Vilitex VBS-13DS) (68 kHz; two 45 mm transducers). After treatment, the foil sheets were removed, rinsed with distilled water, dried at $50 \text{ }^\circ\text{C}$ in a drying oven, and weighed. Seven replicate runs were performed for each position. Statistical processing of the results was carried out using Statgraphics 18 software. Results are presented as mean \pm standard deviation.

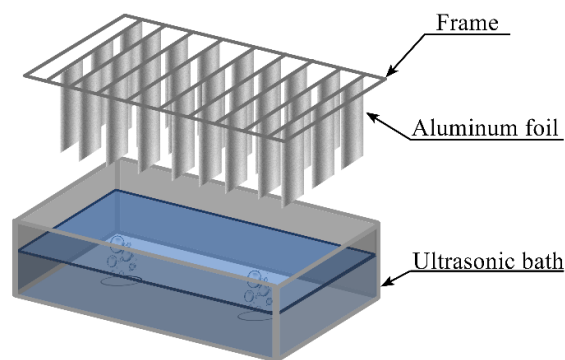


Figure 9. Schematic representation of cavitation mapping setup using aluminum foil in an ultrasonic bath.

3.3. Sonochemical Dispersion of Aluminum Foil in an Ultrasonic Bath

Pre-weighed aluminum foil sheets (3.6×3.3 cm) were clamped in a plastic frame and immersed in a 150 mL glass or plastic vessel containing 100 mL of liquid (distilled water, methanol, ethanol, isopropanol, or DMSO). The vessel was placed in the ultrasonic bath (Ultrasonic cleaner or Vilitex VBS-13DS) with the plane of the foil oriented vertically, parallel to the direction of wave propagation and perpendicular to the pressure node and antinode planes (Figure 10). Ultrasonic treatment was performed under various conditions: power density ($20\text{--}60 \text{ W}\cdot\text{L}^{-1}$), frequency (35 or 68 kHz), treatment time (3–45 min), and temperature ($15\text{--}75 \text{ }^\circ\text{C}$), as specified in the corresponding figure captions and tables. Temperature was maintained using the bath's built-in heater or external cooling as required. After treatment, the foil was removed, rinsed with distilled water, dried at $50 \text{ }^\circ\text{C}$, and weighed. Twelve replicate runs were performed for each set of parameters. Statistical processing of the results was carried out using Statgraphics 18 software. Results are presented as mean \pm standard deviation.

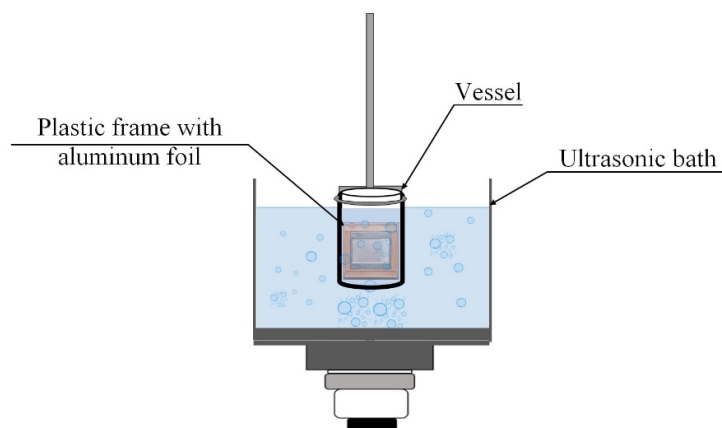


Figure 10. Schematic representation of the setup for sonochemical dispersion of aluminum foil in an ultrasonic bath.

4. Conclusions

In this work, the key parameters of ultrasonic treatment governing the cavitation dose in ultrasonic baths were investigated using aluminum foil mass loss as a quantitative and reproducible metric. All parametric studies were performed at a fixed sample position corresponding to the region of maximum cavitation intensity, ensuring consistent and comparable exposure conditions.

The results demonstrate that dispersion efficiency is governed by a complex interplay between acoustic conditions and the physicochemical properties of the liquid medium, rather than by any single parameter. In addition to ultrasonic frequency and power, the material of the vessel was found to significantly influence the cavitation dose, presumably through its effect on acoustic boundary conditions and energy dissipation at the liquid–solid interface.

A pronounced non-monotonic dependence of cavitation dose on dissolved gas concentration was observed. While moderate gas content promotes cavitation by providing nucleation sites, high gas concentrations ($>50 \text{ mmol}\cdot\text{L}^{-1}$) significantly reduce foil erosion due to the formation of dense cavitation clouds that attenuate ultrasonic wave propagation. Importantly, the investigated parameters are strongly interdependent: increased power and prolonged sonication raise the solvent temperature, which in turn reduces gas solubility and alters cavitation dynamics. This interdependence provides a plausible physical explanation for the stochastic behavior frequently observed in ultrasonic bath experiments.

Contrary to common assumptions, in the present system the addition of surfactants reduced dispersion efficiency, as decreased surface tension disrupts bubble growth and inertial collapse. A complex, non-monotonic temperature dependence was established, with maximum cavitation dose observed at 15 °C and 65 °C. Among the solvents investigated under identical acoustic and geometrical conditions, isopropanol exhibited the highest dispersion efficiency, which can be attributed to its favorable combination of moderate viscosity, high gas solubility, and relatively low saturated vapor pressure, promoting intense mechanical cavitation.

Overall, this study provides a systematic and quantitative assessment of how key experimental parameters—including acoustic conditions, solvent properties, and vessel material—affect the cavitation dose delivered to a sample in an ultrasonic bath. The results contribute to understanding these complex relationships and offer practical guidelines for improving reproducibility and optimizing cavitation-assisted dispersion processes.

Author Contributions: Conceptualization, D.N. and S.S.; methodology, S.S.; software, A.K.; validation, S.S., D.N.; formal analysis, D.N., S.S. A.K; investigation, D.N.; writing—original draft preparation, S.S., D.N. A.K; writing—review and editing, S.S.; visualization, A.K.; supervision, S.S.; project administration, S.S. All authors have read and agreed to the published version of the manuscript.

Funding: This research was funded by the Government Assignment to the Institute of Chemistry and Chemical Engineering, Siberian Branch of the Russian Academy of Sciences (project No. FWES-2026-0004).

Data Availability Statement: Not applicable.

Acknowledgments: This research was carried out using the equipment of Krasnoyarsk Regional Center of Research Equipment of Federal Research Center “Krasnoyarsk Science Center SB RAS” and Center for Collective Use “Science-intensive methods of research and analysis of new materials, nano-materials and mineral raw materials” of Siberian Federal University.

Conflicts of Interest: The authors declare no conflict of interest. The funders had no role in the design of the study; in the collection, analyses, or interpretation of data; in the writing of the manuscript; or in the decision to publish the results.

Abbreviations

The following abbreviations are used in this manuscript:

DMSO	Dimethyl sulfoxide
SDS	sodium dodecyl sulfate

References

1. Wu, P.; Wang, X.; Lin, W.; Bai, L. Acoustic Characterization of Cavitation Intensity: A Review. *Ultrason. Sonochem.* **2022**, *82*, 105878, doi:10.1016/j.ultsonch.2021.105878.
2. Wood, R.J.; Lee, J.; Bussemaker, M.J. A Parametric Review of Sonochemistry: Control and Augmentation of Sonochemical Activity in Aqueous Solutions. *Ultrason. Sonochem.* **2017**, *38*, 351–370, doi:10.1016/j.ultsonch.2017.03.030.
3. Fernandez Rivas, D.; Cintas, P.; Glassey, J.; Boffito, D.C. Ultrasound and Sonochemistry Enhance Education Outcomes: From Fundamentals and Applied Research to Entrepreneurial Potential. *Ultrason. Sonochem.* **2024**, *103*, 106795, doi:10.1016/j.ultsonch.2024.106795.
4. Priyadarshi, A.; Khavari, M.; Subroto, T.; Conte, M.; Prentice, P.; Pericleous, K.; Eskin, D.; Durodola, J.; Tzanakis, I. On the Governing Fragmentation Mechanism of Primary Intermetallics by Induced Cavitation. *Ultrason. Sonochem.* **2021**, *70*, 105260, doi:10.1016/j.ultsonch.2020.105260.
5. Wang, F.; Tzanakis, I.; Eskin, D.; Mi, J.; Connolly, T. In Situ Observation of Ultrasonic Cavitation-Induced Fragmentation of the Primary Crystals Formed in Al Alloys. *Ultrason. Sonochem.* **2017**, *39*, 66–76, doi:10.1016/j.ultsonch.2017.03.057.
6. Anandan, S.; Lana-Villarreal, T.; Wu, J.J. Sonochemical Synthesis of Mesoporous NiTiO₃ Ilmenite Nanorods for the Catalytic Degradation of Tergitol in Water. *Ind. Eng. Chem. Res.* **2015**, *54*, 2983–2990, doi:10.1021/acs.iecr.5b00027.
7. Nazrul Islam, M.; Van Phong, L.; Jeong, J.-R.; Kim, C. A Facile Route to Sonochemical Synthesis of Magnetic Iron Oxide (Fe₃O₄) Nanoparticles. *Thin Solid Films* **2011**, *519*, 8277–8279, doi:10.1016/j.tsf.2011.03.108.
8. Baykal, A.; Kavay, H.; Durmuş, Z.; Demir, M.; Kazan, S.; Topkaya, R.; Toprak, M. Sonochemical Synthesis and Characterization of Mn₃O₄ Nanoparticles. *Open Chem.* **2010**, *8*, 633–638, doi:10.2478/s11532-010-0037-8.
9. Watt, J.; Austin, M.J.; Simocko, C.K.; Pete, D. V.; Chavez, J.; Ammerman, L.M.; Huber, D.L. Formation of Metal Nanoparticles Directly from Bulk Sources Using Ultrasound and Application to E-Waste Upcycling. *Small* **2018**, *14*, 1–8, doi:10.1002/smll.201703615.
10. Muscuso, L.; Cravanzola, S.; Cesano, F.; Scarano, D.; Zecchina, A. Optical, Vibrational, and Structural Properties of MoS₂ Nanoparticles Obtained by Exfoliation and Fragmentation via Ultrasound Cavitation in Isopropyl Alcohol. *J. Phys. Chem. C* **2015**, *119*, 3791–3801, doi:10.1021/jp511973k.
11. Guan, T.; Lu, Y.; Wang, X.; Gilchrist, M.D.; Fang, F.; Zhang, N. Ultrasonics Sonochemistry Scaling up the Fabrication of Wafer-Scale Ni-MoS₂ / WS₂ Nanocomposite Moulds Using Novel Intermittent Ultrasonic-Assisted Dual-Bath. *Ultrason. Sonochem.* **2023**, *95*, 106359, doi:10.1016/j.ultsonch.2023.106359.
12. Pérez-Sánchez, A.; Segura, J.A.; Rubio-Gonzalez, C.; Baldeño-Pérez, L.A.; Soto-Cajiga, J.A. Numerical Design and Analysis of a Langevin Power Ultrasonic Transducer for Acoustic Cavitation Generation. *Sensors Actuators A Phys.* **2020**, *311*, 112035, doi:10.1016/j.sna.2020.112035.
13. Moghtada, A.; Shahrouzianfar, A.; Ashiri, R. Low-Temperature Ultrasound Synthesis of Nanocrystals CoTiO₃ without a Calcination Step: Effect of Ultrasonic Waves on Formation of the Crystal Growth Mechanism. *Adv. Powder Technol.* **2017**, *28*, 1109–1117, doi:10.1016/j.apt.2016.11.004.
14. Basith, M.A.; Ngo, D.-T.; Quader, A.; Rahman, M.A.; Sinha, B.L.; Ahmmad, B.; Hirose, F.; Mølhav, K. Simple Top-down Preparation of Magnetic Bi_{0.9}Gd_{0.1}Fe_{1-x}Ti_xO₃ Nanoparticles by Ultrasonication of Multiferroic Bulk Material. *Nanoscale* **2014**, *6*, 14336–14342, doi:10.1039/C4NR03150D.
15. Jenderka, K.; Koch, C. Investigation of Spatial Distribution of Sound Field Parameters in Ultrasound Cleaning Baths under the Influence of Cavitation. **2006**, *44*, 401–406, doi:10.1016/j.ultras.2006.05.042.
16. Graves, J.E.; Sugden, M.; Litchfield, R.E.; Hutt, D.A.; Mason, T.J.; Cobley, A.J. Ultrasound Assisted Dispersal of a Copper Nanopowder for Electroless Copper Activation. *Ultrason. Sonochem.* **2016**, *29*, 428–438, doi:10.1016/j.ultsonch.2015.10.016.

17. Mermillod-Blondin, F.; Fauvet, G.; Chalamet, A.; Creuzé des Châtelliers, M. A Comparison of Two Ultrasonic Methods for Detaching Biofilms from Natural Substrata. *Int. Rev. Hydrobiol.* **2001**, *86*, 349–360, doi:10.1002/1522-2632(200106)86:3<349:AID-IROH349>3.0.CO;2-B.
18. Hansen, H.E.; Seland, F.; Sunde, S.; Burheim, O.S.; Pollet, B.G. Two Routes for Sonochemical Synthesis of Platinum Nanoparticles with Narrow Size Distribution. *Mater. Adv.* **2021**, *2*, 1962–1971, doi:10.1039/D0MA00909A.
19. Saikova, S.; Nemkova, D.; Krolikov, A.; Pavlikov, A.; Volochaev, M.; Samoilo, A.; Ivanenko, T.; Kuklin, A. Tailoring of Ultrasmall NiMnO₃ Nanoparticles: Optimizing Synthesis Conditions and Solvent Effects. *Molecules* **2024**, *29*, 4846, doi:10.3390/molecules29204846.
20. Saikova, S. V.; Pavlikov, A.Y.; Nemkova, D.I.; Samoilo, A.S.; Karpov, D. V.; Karacharov, A.A.; Novikova, S.A.; Ivanenko, T.Y.; Volochaev, M.N.; Zeer, G.M.; et al. Challenges in Liquid-Phase Exfoliation of Non-van Der Waals Cr₂S₃. *ACS Omega* **2024**, *9*, 46762–46772, doi:10.1021/acsomega.4c02452.
21. Nguyen, V.-T.; Phan, T.-H.; Park, W.-G. Modeling of Shock Wave Produced by Collapse of Cavitation Bubble Using a Fully Conservative Multiphase Model. *Phys. Fluids* **2023**, *35*, 116102, doi:10.1063/5.0167338.
22. Jordens, J.; Appermont, T.; Gielen, B.; Van Gerven, T.; Braeken, L. Sonofragmentation: Effect of Ultrasound Frequency and Power on Particle Breakage. *Cryst. Growth Des.* **2016**, *16*, 6167–6177, doi:10.1021/acs.cgd.6b00088.
23. Dehane, A.; Merouani, S.; Chibani, A.; Hamdaoui, O.; Yasui, K.; Ashokkumar, M. Estimation of the Number Density of Active Cavitation Bubbles in a Sono-Irradiated Aqueous Solution Using a Thermodynamic Approach. *Ultrasonics* **2022**, *126*, 106824, doi:10.1016/j.ultras.2022.106824.
24. Wu, H.; Zheng, H.; Li, Y.; Ohl, C.-D.; Yu, H.; Li, D. Effects of Surface Tension on the Dynamics of a Single Micro Bubble near a Rigid Wall in an Ultrasonic Field. *Ultrason. Sonochem.* **2021**, *78*, 105735, doi:10.1016/j.ultrsonch.2021.105735.
25. Zhao, S.; Yao, C.; Zhang, Q.; Chen, G.; Yuan, Q. Acoustic Cavitation and Ultrasound-Assisted Nitration Process in Ultrasonic Microreactors: The Effects of Channel Dimension, Solvent Properties and Temperature. *Chem. Eng. J.* **2019**, *374*, 68–78, doi:10.1016/j.cej.2019.05.157.
26. Luo, J.; Xu, W.; Zhai, Y.; Zhang, Q. Ultrasonics - Sonochemistry Experimental Study on the Mesoscale Causes of the Influence of Viscosity on Material Erosion in a Cavitation Field. **2019**, *59*, doi:10.1016/j.ultrsonch.2019.104699.
27. Luo, J.; Fu, G.; Xu, W.; Zhai, Y.; Bai, L.; Li, J.; Qu, T. Experimental Study on Attenuation Effect of Liquid Viscosity on Shockwaves of Cavitation Bubbles Collapse. *Ultrason. Sonochem.* **2024**, *111*, 107063, doi:10.1016/j.ultrsonch.2024.107063.
28. Morton, J.A.; Khavari, M.; Qin, L.; Maciejewska, B.M.; Tyurnina, A. V.; Grobert, N.; Eskin, D.G.; Mi, J.; Porfyrakis, K.; Prentice, P.; et al. New Insights into Sono-Exfoliation Mechanisms of Graphite: In Situ High-Speed Imaging Studies and Acoustic Measurements. *Mater. Today* **2021**, *49*, 10–22, doi:10.1016/j.mattod.2021.05.005.
29. Khavari, M.; Priyadarshi, A.; Hurrell, A.; Pericleous, K.; Eskin, D.; Tzanakis, I. Characterization of Shock Waves in Power Ultrasound. *J. Fluid Mech.* **2021**, *915*, R3, doi:10.1017/jfm.2021.186.
30. Kwedi-Nsah, L.-M.; Kobayashi, T. Sonochemical Nitrogen Fixation for the Generation of NO₂⁻ and NO₃⁻ Ions under High-Powered Ultrasound in Aqueous Medium. *Ultrason. Sonochem.* **2020**, *66*, 105051, doi:10.1016/j.ultrsonch.2020.105051.
31. Asakura, Y.; Yasuda, K. Frequency and Power Dependence of the Sonochemical Reaction. *Ultrason. Sonochem.* **2021**, *81*, 105858, doi:10.1016/j.ultrsonch.2021.105858.
32. Knyazeva, A.S.; Krolikov, A.E.; Saikova, S.V. Study of the influence of ultrasonic treatment parameters on processes in the KI–H₂SO₄–H₂O system. *Bulletin of Perm University. CHEMISTRY* **2024**, *14*.
33. Pflieger, R.; Nikitenko, S.I.; Cairós, C.; Mettin, R. *Characterization of Cavitation Bubbles and Sonoluminescence*; SpringerBriefs in Molecular Science; Springer International Publishing: Cham, 2019; ISBN 978-3-030-11716-0.
34. Pflieger, R.; Brau, H.; Nikitenko, S.I. Sonoluminescence from OH(C₂Σ⁺) and OH(A₂Σ⁺) Radicals in Water: Evidence for Plasma Formation during Multibubble Cavitation. *Chem. – A Eur. J.* **2010**, *16*, 11801–11803, doi:10.1002/chem.201002170.

35. Cairós, C.; Mettin, R. Simultaneous High-Speed Recording of Sonoluminescence and Bubble Dynamics in Multibubble Fields. *Phys. Rev. Lett.* **2017**, *118*, 064301, doi:10.1103/PhysRevLett.118.064301.
36. Brothie, A.; Grieser, F.; Ashokkumar, M. Effect of Power and Frequency on Bubble-Size Distributions in Acoustic Cavitation. *Phys. Rev. Lett.* **2009**, *102*, 1–4, doi:10.1103/PhysRevLett.102.084302.
37. Hatanaka, S.I.; Yasui, K.; Kozuka, T.; Tuziuti, T.; Mitome, H. Influence of Bubble Clustering on Multibubble Sonoluminescence. *Ultrasonics* **2002**, *40*, 655–660, doi:10.1016/S0041-624X(02)00193-2.
38. Yamamoto, T.; Okino, S. Ultrasonics Sonochemistry Does Macroscopic Mass Transfer Affect Sonochemical Reaction Rate in An. *Ultrason. Sonochem.* **2025**, *117*, 107361, doi:10.1016/j.ultsonch.2025.107361.
39. Mason, T.J.; Ghimpeteanu, D.; Călinescu, I.; Vinatoru, M.; Trifan, A. A Simple New Approach for Mapping an Ultrasonic Tank for Sonochemistry. *Ultrason. Sonochem.* **2024**, *107*, 106940, doi:10.1016/j.ultsonch.2024.106940.
40. Kuchinskiy, M.; Lyubimova, T.; Rybkin, K.; Sadovnikova, A.; Galishevskiy, V. Investigation of Cavitation in NaCl Solutions in a Sonochemical Reactor Using the Foil Test Method. *Fluid Dyn. Mater. Process.* **2024**, *20*, 1093–1102, doi:10.32604/fdmp.2024.050059.
41. Krefting, D.; Mettin, R.; Lauterborn, W. High-Speed Observation of Acoustic Cavitation Erosion in Multibubble Systems. **2004**, *11*, 119–123, doi:10.1016/j.ultsonch.2004.01.006.
42. Haneef, M.; Yaqoob, K.; Adeel Umer, M.; Hussain, Z. A Novel Strategy for Synthesis of Al Powder Comprising of Al Nanoflakes via Ultrasonication of Al Foil. *Ultrason. Sonochem.* **2020**, *61*, 104838, doi:10.1016/j.ultsonch.2019.104838.
43. Rama, T.; Pamidi, K.; Johansson, Ö.; Löfqvist, T.; Shankar, V. Ultrasonics - Sonochemistry Comparison of Two Different Ultrasound Reactors for the Treatment of Cellulose Fibers. **2020**, *62*, doi:10.1016/j.ultsonch.2019.104841.
44. Verhaagen, B.; Fernández Rivas, D. Measuring Cavitation and Its Cleaning Effect. *Ultrason. Sonochem.* **2016**, *29*, 619–628, doi:10.1016/j.ultsonch.2015.03.009.
45. Abdullah, A.; Malaki, M.; Baghizadeh, E. On the Impact of Ultrasonic Cavitation Bubbles. *Proc. Inst. Mech. Eng. Part C J. Mech. Eng. Sci.* **2012**, *226*, 681–694, doi:10.1177/0954406211414769.
46. Bredihin, S.A.; Andreev, V.N.; Martekha, A.N.; Schenzle, M.G.; Korotkiy, I.A. Erosion Potential of Ultrasonic Food Processing. *Foods Raw Mater.* **2021**, *9*, 335–344, doi:10.21603/2308-4057-2021-2-335-344.
47. Dular, M.; Delgosha, O.C.; Petkovšek, M. Observations of Cavitation Erosion Pit Formation. *Ultrason. Sonochem.* **2013**, *20*, 1113–1120, doi:10.1016/j.ultsonch.2013.01.011.
48. Maksimov, M.A.; Prusakova, V.N. Polypropylene and Propylene Copolymers; Standards Publishing House: Moscow, 2002.
49. Khramkov, V.P.; Chugunov, E.A. Materials for the Production and Processing of Glass and Glass Products; Vysshaya Shkola: Moscow, USSR, 1987.
50. Ashokkumar, M. The Characterization of Acoustic Cavitation Bubbles – An Overview. *Ultrason. Sonochem.* **2011**, *18*, 864–872, doi:10.1016/j.ultsonch.2010.11.016.
51. Baranchikov, A.E.; Ivanov, V.K.; Tretyakov, Y.D. Sonochemical Synthesis of Inorganic Materials. *Russian Chemical Reviews* 2007, *76*, 1–22.
52. Ferrell, G.W.; Crum, L.A. A Novel Cavitation Probe Design and Some Preliminary Measurements of Its Application to Megasonic Cleaning. *J. Acoust. Soc. Am.* **2002**, *112*, 1196–1201, doi:10.1121/1.1498856.
53. Hauptmann, M.; Brems, S.; Camerotto, E.; Zijlstra, A.; Doumen, G.; Bearda, T.; Mertens, P.W.; Lauriks, W. Influence of Gasification on the Performance of a 1 MHz Nozzle System in Megasonic Cleaning. *Microelectron. Eng.* **2010**, *87*, 1512–1515, doi:10.1016/j.mee.2009.11.061.
54. Rooze, J.; Rebrov, E. V.; Schouten, J.C.; Keurentjes, J.T.F. Dissolved Gas and Ultrasonic Cavitation – A Review. *Ultrason. - Sonochemistry* **2013**, *20*, 1–11, doi:10.1016/j.ultsonch.2012.04.013.
55. Jüschke, M.; Koch, C. Model Processes and Cavitation Indicators for a Quantitative Description of an Ultrasonic Cleaning Vessel: Part I: Experimental Results. *Ultrason. Sonochem.* **2012**, *19*, 787–795, doi:10.1016/j.ultsonch.2011.12.020.
56. Raman, V.; Abbas, A. Experimental Investigations on Ultrasound Mediated Particle Breakage. *Ultrason. Sonochem.* **2008**, *15*, 55–64, doi:10.1016/j.ultsonch.2006.11.009.
57. Tokunaga, J. Oxygen, Nitrogen, and Carbon Dioxide in Aqueous. *J. Chem Engin Data* **1975**, *20*, 41–46.

58. Riesz, P.; Berdahl, D.; Christman, C.L. Free Radical Generation by Ultrasound in Aqueous and Nonaqueous Solutions. *Environ. Health Perspect.* **1985**, *64*, 233–252, doi:10.1289/ehp.8564233.
59. Choi, J.; Yoon, S.; Son, Y. Ultrasonics Sonochemistry Effects of Alcohols and Dissolved Gases on Sonochemical Generation of Hydrogen in a 300 KHz Sonoreactor. *Ultrason. Sonochem.* **2023**, *101*, 106660, doi:10.1016/j.ultsonch.2023.106660.

Disclaimer/Publisher's Note: The statements, opinions and data contained in all publications are solely those of the individual author(s) and contributor(s) and not of MDPI and/or the editor(s). MDPI and/or the editor(s) disclaim responsibility for any injury to people or property resulting from any ideas, methods, instructions or products referred to in the content.